Risk-Managed Local Electricity Markets for Unbalanced Distribution Networks: Mellin–Kind DLMP Modeling and Phase-Specific Contracts

Mohammad Reza Karimi Gharigh
School of EECS
KTH Royal Institute of Technology
Stockholm, Sweden
mrkg@kth.se

Mohammad Reza Hesamzadeh
School of EECS
KTH Royal Institute of Technology
Stockholm, Sweden
mrhesa@kth.se

György Dán
School of EECS
KTH Royal Institute of Technology
Stockholm, Sweden
gyuri@kth.se

***Abstract*—This paper proposes a phase-specific risk-management framework for local electricity markets for unbalanced distribution networks with high distributed energy resource (DER) penetration. The delivery-stage market is modeled as a welfare-maximizing quadratically constrained quadratic program (QCQP) with three-phase unbalanced power flow, yielding distribution-level locational marginal prices (DLMPs). DLMP uncertainty is captured using a point-estimate method combined with a Mellin-kind expansion, enabling accurate probability density function (PDF) approximation with few QCQP evaluations. Based on these PDFs, we design phase-specific contracts for local electricity market actors that hedge temporal, spatial, and phase-dependent DLMP volatility while preserving revenue adequacy. Numerical results on a modified unbalanced IEEE 13-node feeder show effective stabilization of flexibility service provider (FSP) and distribution network operator (DNO) revenues.**

***Index Terms*—Local Electricity Market, Unbalanced Distribution Systems, Hedge Contract, Distribution Locational Marginal Prices, Mellin-kind expansion**

I. Introduction

DISTRIBUTED energy resources (DERs), such as rooftop solar panels, smart appliances, and electric vehicles, are transforming distribution systems into dynamic, interactive marketplaces [1]. In this setting, local electricity markets (LEMs) have emerged as a promising structure to coordinate DERs. Unlike traditional operation, LEMs rely on distribution-level locational marginal prices (DLMPs) to signal congestion, voltage deviations, losses, and phase imbalances [2], [3]. However, as DERs and LEMs proliferate, DLMPs in unbalanced networks can exhibit high volatility in time, location (nodes), and across phases [4]. For flexibility service providers (FSPs) and distribution network operators (DNOs), this volatility translates into significant financial risk, which may deter risk-averse actors from market participation [5].

Recent works have explored local hedge contracts for risk management. In [6], a bi-level stochastic pricing model with CVaR is proposed for retailers managing prosumers, while [7] characterizes optimal contracts under contractible uncertainty and derives conditions under which risk can be perfectly hedged. Practical hedging mechanisms such as profile-based tariffs [8], futures-based strategies [9], and bilateral contracts [10] have been shown to improve price stability and consumer protection, while tariff innovation and transparency are arguably important for engagement [11]. Nonetheless, most existing approaches assume phase loads are balanced and prices are uniform, and therefore do not address the spatio-temporal and phase-dependent DLMP volatility inherent to LEMs with unbalanced distribution networks (UDNs).

To address this gap, this paper proposes a phase-specific hedge contract design for LEMs with UDNs. Building on probabilistic DLMP modeling and a welfare-maximizing quadratically constrained quadratic program (QCQP), we: (1) develop a point-estimate-based approach combined with a Mellin-kind expansion to approximate the PDFs of key random variables (DLMPs and substation power) with far fewer samples than Monte Carlo simulation; (2) propose phase-specific FSP contracts (PSFCs) that hedge FSPs against temporal DLMP volatility at the phase level; and (3) derive phase-specific network contracts (PSNCs) that hedge the DNO against spatial and phase-dependent DLMP volatility, enabling risk-averse actors to participate in LEMs with UDNs with predictable financial exposure.

The remainder of the paper is organized as follows. Section II presents the proposed three-stage LEMs with UDNs. Section III introduces the point-estimate-based approach for DLMP density function estimation using a Mellin-kind expansion. Section IV details the proposed hedge contracts for FSPs and the DNO, as offered by the risk management operator (RMO). Section V reports numerical results and validates the proposed hedge contracts, and Section VI concludes the paper.

II. Three-stage LEM Design

We propose a risk-managed three-stage LEM design tailored to UDNs. The market comprises three types of participants: (i) FSPs, (ii) a DNO, both of which are assumed to be risk-averse, and (iii) an RMO, who acts as a risk-taking entity. The key idea is to separate the physical operation of the network from financial risk bearing: the DNO focuses on efficient operation and market clearing under unbalanced network constraints,

979-8-3315-8138-1

while the RMO aggregates and absorbs DLMP-related risks on behalf of risk-averse participants. The proposed LEM design operates over three sequential stages. In the first stage, the risk-management stage (ahead of delivery), the RMO offers PSFCs to FSPs and PSNCs to the DNO to hedge the volatility of FSP surpluses (FSs) and the DNO merchandising surplus (MS), respectively. Each contract specifies by strike prices, contracted volumes, activation periods, and a contract fee for each node and phase. By entering into PSFCs and PSNCs, FSPs and the DNO lock in their expected FSs and MS, transferring DLMP-driven surplus volatility to the RMO in exchange for a risk premium. Contract design and pricing are detailed in Section IV.

In the second stage, the delivery stage, FSPs submit phase-specific bids and offers representing flexibility from local generation and load. The DNO, as the LEM operator, solves a convex surrogate of the QCQP market-clearing problem[1] that captures three-phase unbalanced power flow, network constraints, and the submitted bid/offer functions. The solution yields the dispatch of generators and loads and the nodal, phase-specific DLMPs reflecting congestion, losses, voltage limits, and phase imbalance. Since this problem involves sources of uncertainty, the outcomes become random variables (e.g., FSs, MS, and substation power), whose distributions are approximated as described in Section III.

Finally, in the settlement stage, the RMO uses realized DLMPs and dispatch outcomes to settle the cash flows of signed PSFCs and PSNCs. For each participant, settlement equals the difference between the realized surplus (implied by DLMPs) and the contracted expected surplus defined in the risk-management stage; accordingly, the RMO pays or invoices the participant. Thus, the RMO absorbs gains and losses driven by DLMP volatility, while FSPs and the DNO obtain stabilized, contract-based financial outcomes. Overall, the three-stage design separates physical dispatch from financial risk bearing and enables predictable exposure in LEMs with UDNs.

III. Probabilistic DLMP Modeling

As discussed before, FSPs submit to the LEM their flexibility services, i.e., the supply and demand curves of local generation and load units, and the DNO solves a welfare maximization problem that considers unbalanced power flow equations, technical constraints, and the bid and offer curves submitted by the FSPs. The market-clearing problem at the delivery stage is formulated as the following QCQP:

$$\mathbf{W}^{\text{QCQP}} = \max_{\Xi_{\text{QCQP}}} \sum_{d \in \Omega^{\mathcal{D}}} \mathbf{U}_d \left(P_d^{\mathcal{D}}\right) - \sum_{g \in \Omega^{\mathcal{G}}} \mathbf{C}_g \left(P_g^{\mathcal{G}}\right) \tag{1a}$$

subject to:

$$V_{s_l,\phi}^{\mathfrak{R}} - V_{o_l,\phi}^{\mathfrak{R}} = \sum_{\phi' \in \Omega_l^{\Phi\mathcal{L}}} \left[r_{l,\phi,\phi'} I_{l,\phi'}^{\mathcal{L}\mathfrak{R}} - x_{l,\phi,\phi'} I_{l,\phi'}^{\mathcal{L}\mathfrak{I}}\right], \quad \forall l \in \Omega^{\mathcal{L}}, \phi \in \Omega_l^{\Phi\mathcal{L}}, \tag{1b}$$

$$V_{s_l,\phi}^{\mathfrak{I}} - V_{o_l,\phi}^{\mathfrak{I}} = \sum_{\phi' \in \Omega_l^{\Phi\mathcal{L}}} \left[x_{l,\phi,\phi'} I_{l,\phi'}^{\mathcal{L}\mathfrak{R}} + r_{l,\phi,\phi'} I_{l,\phi'}^{\mathcal{L}\mathfrak{I}}\right], \quad \forall l \in \Omega^{\mathcal{L}}, \phi \in \Omega_l^{\Phi\mathcal{L}}, \tag{1c}$$

$$\sum_{l \in \Omega_{n,\phi}^{\mathcal{L}+}} I_{l,\phi}^{\mathcal{L}\mathfrak{R}} - \sum_{l \in \Omega_{n,\phi}^{\mathcal{L}-}} I_{l,\phi}^{\mathcal{L}\mathfrak{R}} = I_{n,\phi}^{\mathcal{N}\mathfrak{R}}, \; \forall n \in \Omega^{\mathcal{N}}, \phi \in \Omega_n^{\Phi\mathcal{N}}, \tag{1d}$$

$$\sum_{l \in \Omega_{n,\phi}^{\mathcal{L}+}} I_{l,\phi}^{\mathcal{L}\mathfrak{I}} - \sum_{l \in \Omega_{n,\phi}^{\mathcal{L}-}} I_{l,\phi}^{\mathcal{L}\mathfrak{I}} = I_{n,\phi}^{\mathcal{N}\mathfrak{I}}, \; \forall n \in \Omega^{\mathcal{N}}, \phi \in \Omega_n^{\Phi\mathcal{N}}, \tag{1e}$$

$$\sum_{\phi \in \Omega_l^{\Phi\mathcal{L}}} I_{l,\phi}^{\mathcal{L}\mathfrak{R}} = 0, \; \forall l \in \Omega^{\mathcal{L}}, \tag{1f}$$

$$\sum_{\phi \in \Omega_l^{\Phi\mathcal{L}}} I_{l,\phi}^{\mathcal{L}\mathfrak{I}} = 0, \; \forall l \in \Omega^{\mathcal{L}}, \tag{1g}$$

$$\sum_{g \in \Omega_{n,\phi}^{\mathcal{G}}} P_g^{\mathcal{G}} - \sum_{d \in \Omega_{n,\phi}^{\mathcal{D}}} P_d^{\mathcal{D}} = \left(V_{n,\phi}^{\mathfrak{R}} - V_{n,N}^{\mathfrak{R}}\right) I_{n,\phi}^{\mathcal{N}\mathfrak{R}} + \left(V_{n,\phi}^{\mathfrak{I}} - V_{n,N}^{\mathfrak{I}}\right) I_{n,\phi}^{\mathcal{N}\mathfrak{I}}, \; \forall n \in \Omega^{\mathcal{N}}, \phi \in \Omega_n^{\Phi\mathcal{N}} \backslash \{N\}, \tag{1h}$$

$$\sum_{g \in \Omega_{n,\phi}^{\mathcal{G}}} Q_g^{\mathcal{G}} - \sum_{d \in \Omega_{n,\phi}^{\mathcal{D}}} Q_d^{\mathcal{D}} = \left(V_{n,\phi}^{\mathfrak{I}} - V_{n,N}^{\mathfrak{I}}\right) I_{n,\phi}^{\mathcal{N}\mathfrak{R}} - \left(V_{n,\phi}^{\mathfrak{R}} - V_{n,N}^{\mathfrak{R}}\right) I_{n,\phi}^{\mathcal{N}\mathfrak{I}}, \; \forall n \in \Omega^{\mathcal{N}}, \phi \in \Omega_n^{\Phi\mathcal{N}} \backslash \{N\}, \tag{1i}$$

$$\bar{Q}_d^{\mathcal{D}} P_d^{\mathcal{D}} - \bar{P}_d^{\mathcal{D}} Q_d^{\mathcal{D}} = 0, \; \forall d \in \Omega^{\mathcal{D}}, \tag{1j}$$

$$\underline{P}_g^{\mathcal{G}} \leqslant P_g^{\mathcal{G}} \leqslant \bar{P}_g^{\mathcal{G}}, \; \forall g \in \Omega^{\mathcal{G}}, \tag{1k}$$

$$\underline{Q}_g^{\mathcal{G}} \leqslant Q_g^{\mathcal{G}} \leqslant \bar{Q}_g^{\mathcal{G}}, \; \forall g \in \Omega^{\mathcal{G}}, \tag{1l}$$

$$\underline{P}_d^{\mathcal{D}} \leqslant P_{d,}^{\mathcal{D}} \leqslant \bar{P}_d^{\mathcal{D}}, \; \forall d \in \Omega^{\mathcal{D}}, \tag{1m}$$

$$\underline{Q}_d^{\mathcal{D}} \leqslant Q_d^{\mathcal{D}} \leqslant \bar{Q}_d^{\mathcal{D}}, \; \forall d \in \Omega^{\mathcal{D}}, \tag{1n}$$

$$\underline{V}_{n,\phi}^2 \leqslant \left(V_{n,\phi}^{\mathfrak{R}}\right)^2 + \left(V_{n,\phi}^{\mathfrak{I}}\right)^2 \leqslant \bar{V}_{n,\phi}^2, \; \forall n \in \Omega^{\mathcal{N}}, \phi \in \Omega_n^{\Phi\mathcal{N}}, \tag{1o}$$

$$\left(I_{l,\phi}^{\mathcal{L}\mathfrak{R}}\right)^2 + \left(I_{l,\phi}^{\mathcal{L}\mathfrak{I}}\right)^2 \leqslant \bar{I}_{l,\phi}^2, \; \forall l \in \Omega^{\mathcal{L}}, \phi \in \Omega_l^{\Phi\mathcal{L}}, \tag{1p}$$

$$V_{1,\phi}^{\mathfrak{R}} = V_{\phi}^{\mathfrak{R}0}, \phi \in \Omega_1^{\Phi\mathcal{N}}, \tag{1q}$$

$$V_{1,\phi}^{\mathfrak{I}} = V_{\phi}^{\mathfrak{I}0}, \phi \in \Omega_1^{\Phi\mathcal{N}}, \tag{1r}$$

$$\bigcup_{k \in \Omega^{\mathcal{K}}} \Omega_k^{\mathcal{D}} := \Omega^{\mathcal{D}}, \bigcup_{k \in \Omega^{\mathcal{K}}} \Omega_k^{\mathcal{G}} := \Omega^{\mathcal{G}}, \tag{1s}$$

$$\Omega_k^{\mathcal{D}} \cap \Omega_{k'}^{\mathcal{D}} := \varnothing, \Omega_k^{\mathcal{G}} \cap \Omega_{k'}^{\mathcal{G}} := \varnothing, \; \forall k \neq k', k, k' \in \Omega^{\mathcal{K}}. \tag{1t}$$

In (1), the decision vector Ξ_{QCQP} collects active and reactive injections of local load and generation units, local node voltages, and distribution line currents in the three-phase UDN. The objective (1a) maximizes social welfare. Constraints (1b)–(1g) enforce UDN Kirchhoff current and voltage laws, while (1h)–(1i) impose nodal active and reactive power balance; the corresponding Lagrange multipliers define the phase-specific DLMPs. Operational limits are modeled via the constant power-factor condition (1j), local generation and load bounds (1k)–(1n), nodal voltage bounds (1o), and distribution line thermal limits (1p), together with the reference-bus conditions (1q)–(1r). Finally, (1s)–(1t) allocate each unit to exactly one FSP.

The DNO solves a convex surrogate of the QCQP (1). In practice, several inputs of this surrogate problem are uncertain, e.g., spot market price and available outputs of intermittent DERs (rooftop solar, small wind units, and diesel generators). Hence, both the optimal dispatch and the associated DLMPs

[1] In practice, any convex surrogate of this QCQP model can be used based on the LEM market time unit (MTU). The suitable convex surrogate and its selection based on LEM MTU is an interesting aspect of this work for future studies.

979-8-3315-8138-1

(Lagrange multipliers) are random variables (RVs). A Monte Carlo benchmark can be used for solving convex surrogate of (1) over many scenarios, but can be computationally expensive for UDN models [3]. We therefore adopt an analytical PDF approximation based on the Mellin-kind expansion [12], which allows flexible kernel choices (beyond Gaussian) and can approximate non-Gaussian DLMP distributions with relatively few terms.

Let X denote a scalar RV of interest derived from the solution of a convex surrogate of (1), for example, a nodal DLMP or the power at the main substation. Let $\theta(x)$ be a suitably chosen kernel PDF with known cumulants $\{\kappa_{\Theta,i}\}_{i\geqslant 1}$. Following [12], provided that the cumulants of X exist for all orders (and the kernel $\theta(\cdot)$ has known cumulants), the PDF $f_X(x)$ can be represented by the Mellin-kind expansion

$$f_X(x) = \left[\sum_{i=0}^{\infty} \mathbf{B}_i\big(\Delta\kappa_1, \Delta\kappa_2, \ldots, \Delta\kappa_i\big)\frac{\big(-D_x x\big)^i}{i!}\right]\theta(x), \quad (2)$$

where $\mathbf{B}_i(\cdot)$ is the ith complete Bell polynomial, $\Delta\kappa_i := \kappa_{X,i} - \kappa_{\Theta,i}$ is the difference between the ith cumulant of X and that of the kernel distribution, and $\big(-D_x x\big)^i\theta(x)$ denotes the ith derivative of $(-x)^i\theta(x)$ with respect to x. In practice, we truncate (2) at order R to obtain $\widehat{f}_X(\cdot)$; the truncated series may require renormalization, and its accuracy depends on (R, θ) and on the shape of the true density function, potentially degrading for heavy-tailed or multimodal DLMPs [12].

A practical challenge in applying (2) is that it requires the cumulants $\{\kappa_{X,i}\}$ of X, which are not available in closed form since X is obtained implicitly from the QCQP surrogate (1). To avoid many Monte Carlo samples, we estimate the first R raw moments of X via a point-estimate method and then recover cumulants using the standard moment–cumulant recursion. Let $\nu_{X,i} := \mathbb{E}[X^i]$ and $\widehat{\nu}_{X,i}$ denote the corresponding moment estimates ($i = 1, \ldots, R$). The cumulants are computed as

$$\kappa_{X,i} = \nu_{X,i} - \sum_{i'=1}^{i-1}\binom{i-1}{i'-1}\kappa_{X,i'}\,\nu_{X,i-i'}, \quad (3)$$

which, together with the kernel cumulants $\{\kappa_{\Theta,i}\}$, yields $\Delta\kappa_i$ and hence $f_X(\cdot)$ via (2) truncated at order R. Algorithm 1 summarizes the procedure.

Algorithm 1 Point-estimate and Mellin-kind expansion for DLMP density function estimation

Require: Network, bids/offers, constraints in (1); uncertain inputs $\boldsymbol{\xi}$ with PDFs; point-estimate set $\{(\boldsymbol{\xi}^{(k)}, w^{(k)})\}_{k=1}^{K}$; expansion order R; kernel PDF $\theta(\cdot)$

Initialize moment accumulators $\widehat{\nu}_{X,i} \leftarrow 0,\ i = 1, \ldots, R$
for $k = 1$ to K **do**
  Set parameters $\boldsymbol{\xi} \leftarrow \boldsymbol{\xi}^{(k)}$
  Solve (convex surrogate of) QCQP (1); obtain $X^{(k)}$
  for $i = 1$ to R **do**
    $\widehat{\nu}_{X,i} \leftarrow \widehat{\nu}_{X,i} + w^{(k)}\left(X^{(k)}\right)^i$
  end for
end for
Compute cumulants $\widehat{\kappa}_{X,i}$ from $\widehat{\nu}_{X,i}$ using (3)
Compute $\Delta\kappa_i \leftarrow \widehat{\kappa}_{X,i} - \kappa_{\Theta,i},\ i = 1, \ldots, R$
return $\widehat{f}_X(\cdot)$ from (2) truncated at R

IV. Hedge Contract Design

In this section, we extend the hedge design proposed in [13] to unbalanced LEMs, explicitly accounting for phase imbalances. The RMO offers: (i) PSFCs to hedge FSPs against temporal DLMP volatility, and (ii) PSNCs to hedge the DNO against spatial and phase-dependent DLMP volatility. Contract prices are computed using the probabilistic DLMP model and the Mellin-kind density function approximation developed in Section III. The surplus of FSP k can be written as

$$\mathbf{FS}_k = \sum_{d\in\Omega_k^{\mathcal{D}}}\left[\mathbf{U}_d(P_d^{\mathcal{D}}) - \lambda^{\mathcal{P}}_{n_d,\phi_d^{\mathcal{D}}}P_d^{\mathcal{D}}\right] + \sum_{g\in\Omega_k^{\mathcal{G}}}\left[\lambda^{\mathcal{P}}_{e_g,\phi_g^{\mathcal{G}}}P_g^{\mathcal{G}} - \mathbf{C}_g(P_g^{\mathcal{G}})\right], \quad (4)$$

where n_d and e_g are the nodes to which load unit d and generation unit g are connected, and $\mathbf{U}_d$ and $\mathbf{C}_g$ are the corresponding utility and cost functions, which are piecewise-linear concave and convex functions, respectively. Moreover, $\lambda^{\mathcal{P}}_{n,\phi}$ is the realized DLMP obtained from solving a convex surrogate of (1) and corresponds to the Lagrange multipliers associated with the active power balance constraints in (1h). Similarly, the DNO's MS can be computed as

$$\mathbf{MS} = \sum_{n\in\Omega^{\mathcal{N}}}\sum_{\phi\in\Omega_n^{\Phi\mathcal{N}}}\left[\sum_{d\in\Omega^{\mathcal{D}}_{n,\phi}}\lambda^{\mathcal{P}}_{n,\phi}P_d^{\mathcal{D}} - \sum_{g\in\Omega^{\mathcal{G}}_{n,\phi}}\lambda^{\mathcal{P}}_{n,\phi}P_g^{\mathcal{G}}\right]. \quad (5)$$

Both $\mathbf{FS}_k$ and $\mathbf{MS}$ are random variables driven by the DLMP vector and by the solution of the convex surrogate of QCQP in (1).

A. PSFCs between the RMO and FSPs

To hedge temporal DLMP volatility for each phase, the RMO offers a PSFC to each FSP k. The contract replicates the FSP's surplus using a portfolio of standard Cap and Floor contracts written on phase-specific DLMPs, extending the construction in [13] to the unbalanced setting. Formally, a PSFC for FSP k is defined as

$$\mathbf{PSFC}_k := \sum_{d\in\Omega_k^{\mathcal{D}}}\sum_{j\in\Omega^{\mathcal{J}}}\mathbf{Floor}\big(\lambda^{\mathcal{P}}_{n_d,\phi_d^{\mathcal{P}}} \mid S^{\mathcal{D}}_{d,j}, V^{\mathcal{D}}_{d,j}\big) + \sum_{g\in\Omega_k^{\mathcal{G}}}\sum_{j\in\Omega^{\mathcal{J}}}\mathbf{Cap}\big(\lambda^{\mathcal{P}}_{e_g,\phi_g^{\mathcal{G}}} \mid S^{\mathcal{G}}_{g,j}, V^{\mathcal{G}}_{g,j}\big), \quad (6)$$

where $\left(S^{\mathcal{D}}_{d,j}, V^{\mathcal{D}}_{d,j}\right)$ and $\left(S^{\mathcal{G}}_{g,j}, V^{\mathcal{G}}_{g,j}\right)$ are the strike prices and volumes associated with the piecewise-linear bids and offers of the units belonging to FSP k. Here, $\mathbf{Cap}(\lambda \mid S, V) := \max\{\lambda - S, 0\}V$ and $\mathbf{Floor}(\lambda \mid S, V) := \max\{S - \lambda, 0\}V$, and $\mathbf{I}(\cdot)$ denotes the indicator function when needed.

By construction, and under the same assumptions as in [13], one can show that for each realization of DLMPs $\lambda^{\mathcal{P}}_{n,\phi}$, the payoff of the PSFC for FSP k equals the realized FSP surplus, $\mathbf{PSFC}_k = \mathbf{FS}_k$, i.e., the PSFC provides a complete hedge of temporal DLMP volatility for FSP k across all phases.

979-8-3315-8138-1

B. PSNCs between the RMO and the DNO

While PSFCs hedge the FSPs, the DNO remains exposed to spatial and phase-dependent volatility of DLMPs through the $\mathbf{MS}$. To hedge this exposure, the RMO offers PSNCs indexed by node n and phase ϕ, defined with respect to a reference node n' (e.g., the connecting point substation to the upper-level network). Following [13], we use power-loss contribution factors to construct contracts whose payout matches the MS under each realization of DLMPs, and extend this idea to the UDN. The PSNC at node n and phase ϕ with respect to the reference node n' is defined as

$$\mathbf{PSNC}_{n\to n',\phi} := \Big[\lambda^{\mathcal{P}}_{n',\phi}(1-\delta_{n,\phi}) - \lambda^{\mathcal{P}}_{n,\phi}\Big] \sum_{g\in\Omega^{\mathcal{G}}_{n,\phi}} \sum_{j\in\Omega^{\mathcal{J}}} V^{\mathcal{G}}_{g,j}\mathbf{I}(\lambda^{\mathcal{P}}_{n,\phi} \geqslant S^{\mathcal{G}}_{g,j}) + \Big[\lambda^{\mathcal{P}}_{n,\phi} - \lambda^{\mathcal{P}}_{n',\phi}(1+\delta_{n,\phi})\Big] \sum_{d\in\Omega^{\mathcal{D}}_{n,\phi}} \sum_{j\in\Omega^{\mathcal{J}}} V^{\mathcal{D}}_{d,j}\mathbf{I}(\lambda^{\mathcal{P}}_{n,\phi} \leqslant S^{\mathcal{D}}_{d,j}), \tag{7}$$

where $\delta_{n,\phi}$ is the contribution factor of local load and generation units at node n and phase ϕ to total active power losses. These factors must satisfy

$$\sum_{n,\phi} \delta_{n,\phi}\Bigg(\sum_{d\in\Omega^{\mathcal{D}}_{n,\phi}} P^{\mathcal{D}}_{d} + \sum_{g\in\Omega^{\mathcal{G}}_{n,\phi}} P^{\mathcal{G}}_{g}\Bigg) = \sum_{g} P^{\mathcal{G}}_{g} - \sum_{d} P^{\mathcal{D}}_{d}, \tag{8}$$

i.e., the loss contributions allocate the total active power losses, expressed as the net injection of the distribution system. Aggregating PSNCs over all nodes and phases yields the total PSNC payout

$$\mathbf{PSNC} := \sum_{n\in\Omega^{\mathcal{N}}} \sum_{\phi\in\Omega^{\Phi\mathcal{N}}_{n}} \mathbf{PSNC}_{n\to n',\phi}. \tag{9}$$

Using (5) and (9), and following the same arguments as in [13], it can be shown that for each realization of DLMPs, $\mathbf{PSNC} = \mathbf{MS}$, i.e., the aggregated PSNC payout equals the realized MS, providing a complete hedge of spatial and phase-dependent DLMP volatility for the DNO. Note that, for each DLMP realization, the aggregate payout of all PSFCs and PSNCs equals the optimal social welfare obtained from the convex surrogate dispatch model, so the contracts merely redistribute FS and MS while keeping the LEM revenue-adequate and financially balanced.

V. Numerical Results

We evaluate the proposed phase-specific hedge design on a modified unbalanced IEEE 13-node feeder [14]. The feeder is a three-phase, four-wire radial network (4.16 kV, 1 MVA base) with 14 single-phase loads totaling 3,286 kW and additional DERs: three single-phase PV units, two single-phase wind-turbine (WT) units, and three three-phase diesel-generator (DG) units (rated at 150, 300, and 200 kW, respectively). All resources are assigned to five FSPs as shown in Fig. 1. Uncertainty in the spot market price, PV availability, and WT availability is modeled using Weibull, Beta, and Weibull distributions, respectively.

As discussed in Section III, the PDFs of the variables in the market-clearing problem (1) can be obtained via a Monte

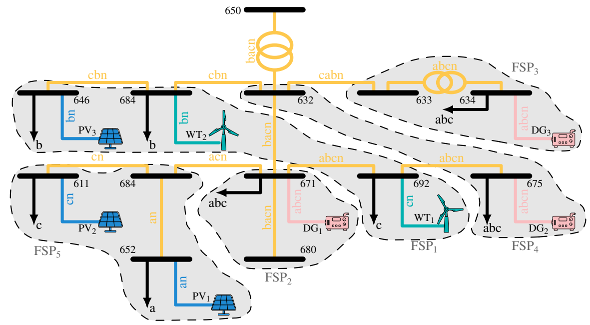

Fig. 1. The modified IEEE 13-node distribution network

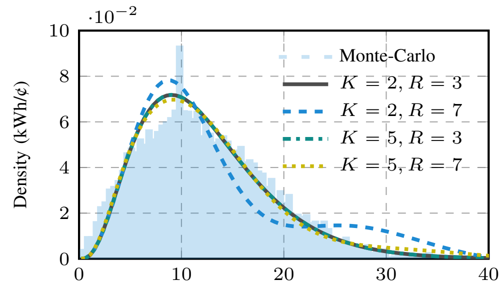

Fig. 2. The PDFs of active DLMPs at local node 671 phase A.

Carlo simulation. For benchmarking, we first generate 1,000 samples of the uncertain parameters and solve (1) for each realization. The resulting empirical PDF of the DLMP at node 671, phase A, is depicted in Fig. 2 (histogram). Note that this approach is computationally expensive; the computations take approximately 371 hours for our case study on a laptop with an Apple M3 Pro processor and 36 GB of RAM.

We then apply the proposed point-estimate method. Specifically, we solve a convex surrogate of (1) for K weighted deterministic realizations of the uncertain inputs using a moment-matching point-estimate method, $\{(\boldsymbol{\xi}^{(k)}, w^{(k)})\}_{k=1}^{K}$. In particular, we use the 2-point and 5-point versions of the point-estimate method (2-PEM and 5-PEM), yielding a joint weighted point set $\{(\boldsymbol{\xi}^{(k)}, w^{(k)})\}_{k=1}^{K}$ for the m uncertain inputs. Using the resulting decision variables and Lagrange multipliers (including DLMPs), we approximate the low-order moments of the DLMPs and compute the corresponding cumulants via (3). Next, we estimate the PDF of the DLMP at node 671, phase A, using the Mellin-kind expansion (2) truncated at order $R \in \{3, 7\}$ with a Gamma kernel $\theta(\cdot)$, parameterized by moment matching (i.e., matched to the mean and variance of the chosen RV).

Fig. 2 reports the resulting approximations for different values of (K, R) (solid lines). The Mellin-kind expansion combined with the point-estimate method closely matches the Monte Carlo benchmark as (K, R) increases, indicating that the DLMP density function can be captured accurately with far fewer QCQP evaluations than Monte Carlo. In our case study, finding the DLMP density function required at most 111 minutes (for the largest (K, R)), compared to approximately 371 hours for the Monte Carlo benchmark with 1,000 samples. The estimated density function $\widehat{f}_{\lambda}(\cdot)$ is then used to price the hedge contracts in Section IV; in particular,

979-8-3315-8138-1

TABLE I
THE FSS, MS, AND PAYOUT OF PSFC AND PSNC IN THE MODIFIED UNBALANCED IEEE 13-NODE SYSTEM

t	$\mathbf{FS}_1$ ($/h)	$\mathbf{PSFC}_1$ ($/h)	$\mathbf{FS}_2$ ($/h)	$\mathbf{PSFC}_2$ ($/h)	$\mathbf{FS}_3$ ($/h)	$\mathbf{PSFC}_3$ ($/h)	$\mathbf{FS}_4$ ($/h)	$\mathbf{PSFC}_4$ ($/h)	$\mathbf{FS}_5$ ($/h)	$\mathbf{PSFC}_5$ ($/h)	$\mathbf{MS}$ ($/h)	$\mathbf{PSNC}$ ($/h)
1	369.29	365.54	489.08	489.08	835.96	837.11	610.38	610.03	262.67	260.10	0.80	1.05
2	360.98	359.66	486.19	486.38	808.99	809.33	590.79	590.87	260.21	259.67	1.87	2.20
3	348.93	349.35	478.95	478.95	780.11	780.54	569.27	569.69	252.34	252.34	2.17	2.48
4	339.82	339.91	475.86	475.86	755.11	755.21	550.85	550.94	247.67	247.67	2.77	2.92
5	331.17	331.17	472.78	472.78	730.46	730.47	532.86	532.87	243.01	243.01	2.94	3.22
6	323.52	323.53	468.85	468.85	705.82	705.83	515.29	515.30	238.21	238.21	2.98	3.19
7	317.18	317.18	467.64	467.64	681.56	681.57	498.48	498.50	232.59	232.59	2.99	3.22
8	312.17	312.18	468.30	468.30	656.53	656.53	481.80	481.80	227.05	227.05	2.69	2.84
9	309.08	309.09	468.22	468.22	629.74	629.76	464.90	464.92	220.40	220.40	2.35	2.51
10	309.38	309.39	470.59	470.59	602.04	602.06	448.94	448.96	211.66	211.66	1.90	2.12
11	317.52	317.52	468.52	468.52	567.57	567.57	432.27	432.27	200.94	200.94	1.78	2.01
$\mathbb{E}(.)$	335.85	335.46	475.34	475.36	735.22	735.43	537.56	537.62	243.43	243.16	2.43	2.67

the required expectations for Caps and Floors are computed under $\widehat{f}_\lambda(\cdot)$, i.e., $\mathbb{E}\left(\lambda^{\mathcal{P}}_{n,\phi} \mid \lambda^{\mathcal{P}}_{n,\phi} \gtreqless S\right)$, and used to determine the contract fees.

Next, we evaluate the effectiveness of the proposed hedge contracts for the modified 13-node unbalanced system. The contract fees are determined using the probability density obtained from the proposed density-function estimation method. Then, to evaluate realized outcomes under uncertainty, we use a Monte Carlo simulation. Since it is not practical to present contract payoffs over all Monte Carlo scenarios, we select 11 representative market realizations by reducing the original scenario set using a scenario reduction approach similar to [15]. For this reduced set of scenarios, the realized surpluses and the corresponding hedge contract payoffs for the five FSPs and the DNO are reported in Table I.

As shown in Table I, the payoff of each contract closely matches the realized surplus under each scenario, confirming that PSFCs and PSNCs replicate the underlying FS and MS quantities. This indicates that the proposed hedge contracts are fairly priced in expectation while providing effective protection against DLMP volatility for the FSPs and the DNO. Moreover, using the scenario probabilities, the pre-hedge surplus variances are $\mathrm{Var}(\mathbf{FS}_1) = 351.68$, $\mathrm{Var}(\mathbf{FS}_2) = 50.82$, $\mathrm{Var}(\mathbf{FS}_3) = 3944.22$, $\mathrm{Var}(\mathbf{FS}_4) = 1957.74$, $\mathrm{Var}(\mathbf{FS}_5) = 181.00$, and $\mathrm{Var}(\mathbf{MS}) = 0.3945$ in $(\$/\mathrm{h})^2$. After hedging, the residual surplus volatility is substantially reduced, i.e., $\mathrm{Var}(\mathbf{FS}_1 - \mathbf{PAFC}_1) = 1.207$, $\mathrm{Var}(\mathbf{FS}_2 - \mathbf{PAFC}_2) = 0.004$, $\mathrm{Var}(\mathbf{FS}_3 - \mathbf{PAFC}_3) = 0.101$, $\mathrm{Var}(\mathbf{FS}_4 - \mathbf{PAFC}_4) = 0.032$, $\mathrm{Var}(\mathbf{FS}_5 - \mathbf{PAFC}_5) = 0.488$, and $\mathrm{Var}(\mathbf{MS} - \mathbf{PANC}) = 0.0041$ in $(\$/\mathrm{h})^2$, confirming stabilization of FSP and DNO revenues against DLMP volatility, consistent with the close tracking between surpluses and contract payoffs in Table I.

VI. CONCLUSION

This paper proposed a phase-specific risk-management framework for LEMs with UDNs, combining a three-stage market design, a welfare-maximizing UDN, and a point-estimate-based Mellin-kind expansion for DLMP density function estimation. Based on the calculated PDFs, we introduced PSFCs for FSPs and PSNCs for the DNO that hedge temporal, spatial, and phase-dependent DLMP volatility while preserving revenue adequacy. Numerical results on a modified unbalanced IEEE 13-node feeder show that the proposed density function approximation closely matches Monte Carlo benchmarks and that the contracts effectively stabilize the financial outcomes of FSPs and the DNO.

REFERENCES

[1] M. Adham, S. Keene, and R. B. Bass, "Distributed energy resources: A systematic literature review," *Energy Reports*, vol. 13, pp. 1980–1999, 2025.

[2] X. Wang, F. Li, L. Bai, and X. Fang, "DLMP of competitive markets in active distribution networks: Models, solutions, applications, and visions," *Proceedings of the IEEE*, vol. 111, no. 7, pp. 725–743, 2022.

[3] S. Mohammadi, M. R. Hesamzadeh, and D. W. Bunn, "Distribution locational marginal pricing (dlmp) for unbalanced three-phase networks," *IEEE Transactions on Power Systems*, vol. 37, no. 5, pp. 3443–3457, 2021.

[4] Z. Tan, T. Cheng, Y. Liu, and H. Zhong, "Extensions of the locational marginal price theory in evolving power systems: A review," *IET Generation, Transmission & Distribution*, vol. 16, no. 7, pp. 1277–1291, 2022.

[5] T. Chen and F. Vandendriessche, "Enabling independent flexibility service providers to participate in electricity markets: A legal analysis of the belgium case," *Utilities Policy*, vol. 81, 2023.

[6] P. Beraldi and S. Khodaparasti, "Designing electricity tariffs in the retail market: A stochastic bi-level approach," *International Journal of Production Economics*, vol. 257, 2023.

[7] D. R. Biggar and M. R. Hesamzadeh, "Optimal retail contracts with contractible uncertainty," *Energy Economics*, vol. 136, 2024.

[8] C. Winzer, H. Ramírez-Molina, L. Hirth, and I. Schlecht, "Profile contracts for electricity retail customers," *Energy Policy*, vol. 195, 2024.

[9] F. Tanrisever, B. Büke, and G. Jongen, "Futures hedging in electricity retailing," *Annals of Operations Research*, vol. 330, no. 1, pp. 757–785, 2023.

[10] M. Moazzami, H. Shahinzadeh, M. Najafi, Z. Azani, S. Azani, and G. B. Gharehpetian, "Electricity tariff volatility mitigation using uncertainty-diminution and hedge contracts along with risk management policies," in *IEEE International Conference on Electrical Engineering (ICEE)*, 2022, pp. 1063–1068.

[11] H. Hampton, A. Foley, D. F. Del Rio, B. Smyth, D. Laverty, and B. Caulfield, "Customer engagement strategies in retail electricity markets: A comprehensive and comparative review," *Energy Research & Social Science*, vol. 90, 2022.

[12] T. Brenn and S. N. Anfinsen, "A framework for mellin kind series expansion methods," 2017.

[13] D. R. Biggar and M. R. Hesamzadeh, "An integrated theory of dispatch and hedging in wholesale electric power markets," *Energy Economics*, vol. 112, 2022.

[14] D. S. A. Subcommittee, "IEEE 13 node test feeder," IEEE Power & Energy Society, Tech. Rep., 1992, available: https://cmte.ieee.org/pes-testfeeders/resources/.

[15] J. Li, S. Wang, Y. Li, and H. Liu, "Photovoltaic generation scenario reduction method based on improved k-means clustering," in *International Conference on Information Control, Electrical Engineering and Rail Transit*. Springer, 2022, pp. 1–16.